



# Czochralski growth of $\text{Sr}_2\text{Tb}_8(\text{SiO}_4)_6\text{O}_2$ crystals for visible–near IR magneto-optical applications

Xin Chen, Wenhui Zhang, Qiping Wan, Feiyun Guo, Naifeng Zhuang, Hao Fu, Xitong Xie, Jianzhong Chen\*

College of Chemistry and Chemical Engineering, Fuzhou University, Fuzhou 350108, China

## ARTICLE INFO

### Article history:

Received 21 February 2014

Received in revised form 12 May 2014

Accepted 26 May 2014

Available online 21 June 2014

### Keywords:

Silicate

Oxyapatite

Czochralski method

Magneto-optical properties

Faraday isolators

## ABSTRACT

$\text{Sr}_2\text{Tb}_8(\text{SiO}_4)_6\text{O}_2$  crystals have been grown and investigated for the first time for magneto-optical applications. The X-ray powder diffraction confirms that the compound crystallizes in the hexagonal system, with a common oxyapatite structure. The as-grown crystal exhibits low thermal expansion anisotropy ( $\alpha_a/\alpha_c \approx 1.1$ ), and the hardness is about 5.0 Moh. The temperature dependence of the magnetic susceptibility indicated that the  $\text{Sr}_2\text{Tb}_8(\text{SiO}_4)_6\text{O}_2$  crystal exhibits paramagnetic behavior over the experimental temperature-range 2–300 K. The present investigations demonstrate that  $\text{Sr}_2\text{Tb}_8(\text{SiO}_4)_6\text{O}_2$  crystals show a higher visible transparency and a larger Faraday rotation than terbium gallium garnet (TGG) crystals.  $\text{Sr}_2\text{Tb}_8(\text{SiO}_4)_6\text{O}_2$  is therefore a very promising material in particular for new magneto-optical applications in the visible–near IR wavelength region.

© 2014 Elsevier B.V. All rights reserved.

## 1. Introduction

Faraday isolators (FIs) using the non-reciprocity of the Faraday effects are fundamental components used in advanced optical communications and precise optical measurement systems to prevent harmful back-reflections from reaching a laser equipped with such an isolator, and to eliminate parasitic oscillations in amplifier systems or frequency instabilities in laser diodes [1]. As the central part of the FIs, the 45° Faraday rotator obtained by magneto-optic crystals primarily determines the performance of FIs [2]. Yttrium iron garnet,  $\text{Y}_3\text{Fe}_5\text{O}_{12}$  (YIG), and Bi-doped YIG crystals, characterized by a high transparency in the IR region (1.2–5.0  $\mu\text{m}$ ) [3], a large Faraday rotation angle, and a low saturation magnetization, are so far the most commonly used crystals in FIs.

However, as the rapid development of fiber lasers, the demand of optical isolators operated at wavelengths below 1100 nm (i.e. the visible–near IR region of 400–1100 nm) in advanced display systems, high-precision laser measurements, etc., are rapidly increasing, while the conventional YIG and doped YIG are not practical because of their poor transmittance in this spectral region [4]. Therefore soon after the introduction of YIG and doped YIG as optical isolators, an intensive search for new magneto-optic crystals with similarly large Faraday rotation angle but a low optical

absorption loss began and led to numerous new materials based on rare-earth (RE) garnet single crystals. These are optically isotropic thanks to the cubic symmetry, and exhibit Curie–Weiss paramagnetic behavior, due to the  $4f \rightarrow 4f5d$  transition of  $\text{RE}^{3+}$  ions [5].  $\text{Tb}^{3+}$  yields to the largest Faraday rotation, so that electric dipole contribution of  $\text{Tb}^{3+}$  dominates even over that of  $\text{Fe}^{3+}$  in magnetic terbium–iron garnet [6], and hence show the best magneto-optical properties [7,8]. Complex theoretical approaches have been done through the perturbation Hamiltonian, which takes into account the spin–orbit coupling, the crystal field, and the superexchange interaction [9].

Terbium–aluminum garnet,  $\text{Tb}_3\text{Al}_5\text{O}_{12}$  (TAG), has been reported to show the best paramagnetic magneto-optical properties in the visible–near IR spectral region with a high light transmission coefficient and a high Verdet constant [10], nevertheless, its incongruent melting nature and unstable TAG phase in the  $\text{Tb}_2\text{O}_3$ – $\text{Al}_2\text{O}_3$  system have impeded so far the growth of industrially practicable crystals [11]. With the lack of TAG, terbium–gallium garnet,  $\text{Tb}_3\text{Ga}_5\text{O}_{12}$  (TGG) crystal, the next-best magneto-optic material of TAG [12], was introduced as FIs for high-power laser machinery [13], and make up for the deficiency of YIG in the visible and near infrared spectral regions. But although TGG melts congruently at approximately 1825 °C, its Czochralski growth is not exempt of difficulties. The decomposition and evaporation of  $\text{Ga}_2\text{O}_3$  from the TGG melt, which is easy to over flow the container during the crystal growth process due to its large infiltration, lead to a serious component deviation from the congruent melting [14,15].

\* Corresponding author. Tel.: +86 591 22866130; fax: +86 591 22866232.

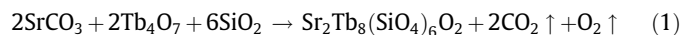
E-mail address: [j.z.chen@fzu.edu.cn](mailto:j.z.chen@fzu.edu.cn) (J. Chen).

Taking into account the requirements for an excellent magneto-optic material applied in the visible–near IR spectral region, the family of oxyapatite-type rare-earth silicates (OTRS), which demonstrate great potential for applications in solid-state lasers [16,17], and phosphors [18], have come to draw more and more attention from our research group. OTRS belong to a wide class of isostructural compounds  $M_{\chi}R_{10-\chi}(\text{SiO}_4)_6\text{O}_2$  (where  $M$  = alkali or alkaline-earth metal, and  $R$  = lanthanide), which crystallize in the hexagonal system with space group  $P6_3/m$ . Interestingly, the crystals have a peculiarity in structure; i.e., the various cations  $M^{2+}$  and  $R^{3+}$  distribute randomly along the 4f sites with similar probabilities, and 6h sites are occupied only by the  $R^{3+}$  ions [19,20]. The sites of 4f and 6h are different in point symmetry, so the  $R^{3+}$  ions locate in different crystal fields. Furthermore, it is worth noting that Toropov et al. [21,22] have reported the phase diagrams for  $\text{Ln}_2\text{O}_3$ – $\text{SiO}_2$  systems ( $\text{Ln} = \text{Y}, \text{La}, \text{Sm}, \text{Gd}, \text{Tb}, \text{Dy}, \text{Er}$  and  $\text{Yb}$ ) in which  $\text{Ln}_8(\text{SiO}_4)_6$  were identified as the apatite phase and melts congruently. Hence, in this investigation, we attempt to employ the Czochralski technique to grow  $\text{Sr}_2\text{Tb}_8(\text{SiO}_4)_6\text{O}_2$  (STS) single crystals, which also has the apatite structure and belongs to the OTRS family. The spectral and magneto-optical properties were discussed as well.

## 2. Experimental

### 2.1. Synthesis and crystal growth

The starting materials used for the single crystal growth were prepared by the conventional solid-state reaction route from stoichiometric mixtures of analar grade  $\text{SrCO}_3$ ,  $\text{SiO}_2$ , and  $\text{Tb}_4\text{O}_7$  powders according to the following chemical reaction equation:



The raw materials were weighted accurately on the basis of stoichiometric ratio with the excess amount 1 wt% of  $\text{SiO}_2$  to compensate for its volatilization loss during the process of crystal growth, and then mixed homogeneously in an alumina mortar with the ethanol. The uniformly mixed raw materials were pressed into tablets under 10 MPa pressure and then sintered at 1100 °C for 12 h in air. They were then cooled to room temperature, reground, and sintered again at 1200 °C in air for 20 h. The purity of the sample was checked by X-ray powder diffraction. A single apatite phase of STS was obtained when repeated heat treatment caused no further changes in the X-ray powder diffraction.

The single crystals STS were grown from the stoichiometric melt by the conventional RF-heating Czochralski technique. The polycrystalline pieces were melted in an iridium crucible (56 mm in diameter and 43 mm in height), heated by a radiofrequency furnace under a protective atmosphere of  $\text{N}_2$ . Since it takes slightly larger current to melt the polycrystalline pieces than that for  $\text{TiO}_2$ , which melts at about 1870 °C [23], the melting temperature of this material is estimated to be in the range 1900–2000 °C. After the starting materials were completely molten, a seed crystal of (001) orientation, cut from the initial STS crystal which obtained by crystallization on the iridium rod, was dipped into the melt and then slowly withdrawn, so that the crystal began to grow along the  $c$ -axis with 0.5–0.7 mm/h pulling rate and 16–25 r/min rotating velocity. After crystallization, the crystal was pulled out of the melt and cooled down to room temperature at a rate of 5–30 K/h.

The as-grown STS single crystal is transparent and crack free with a very slight yellowish coloration. Fig. 1(c) shows one of the as-grown STS with dimensions of  $\varnothing 23 \times 29$  mm. After oriented accurately by X-ray diffraction, the as-grown crystals were cut along the (001) crystal plane, and then wafers were ground and

polished carefully for the following measurement, as shown in Fig. 1(d).

### 2.2. Structure determination

In order to confirm the structure of the as-grown STS crystals, the X-ray powder diffraction (XRD) patterns were recorded using a computer automated diffractometer (Rigaku D/max-3c) equipped with  $\text{Cu K}\alpha$  radiation ( $\lambda = 1.54051 \text{ \AA}$ ) at room temperature. The XRD patterns of the as-grown STS crystals are very similar, so only the pattern of the STS-3 crystal is given in Fig. 2, which agrees well with the standard pattern of STS (PDF 29-1314) without any impurities peaks. This means that all the as-grown crystals are identified to be oxyapatite-type STS crystals, which crystallize in the hexagonal system with space group  $P6_3/m$ . Besides, No evidence for incongruent melting was found according to the X-ray analysis of the residual melt and as-grown crystal, which indicates that the two diffraction patterns were essentially the same and corresponded to that of the single phase of apatite.

### 2.3. Hardness and thermal expansion

The hardness of as-grown STS crystal, determined by using a 401MVA™ Vickers-microhardometer, is about 524.2 VDH, and is equal to about 5.0 Moh, which is close to that of siliceous glass, and hence is favorable for crystal machining. The coefficients of thermal expansion of STS single crystals were evaluated by using a Netzsch DIL402PC model thermo-mechanical analyzer equipment from room temperature to 700 °C at a heating rate of 10 K/min.

### 2.4. Spectral measurement

The wafer shown in Fig. 1(d) was used for the spectral measurement. The transmission spectrum was measured by using a Perkin–Elmer Lambda UV–Vis–NIR spectrophotometer, over the wavelength range from 400 to 1500 nm with a 2 nm resolution at room temperature. In order to evaluate the transparency of as-grown crystal, a commercial device-quality TGG sample, supplied by TCT Co., Ltd. Fuzhou, was also used for the spectral measurement with the same test conditions.

### 2.5. Variable-temperature magnetic susceptibility

The temperature dependence of the magnetic susceptibility was measured under both zero-field-cooled (ZFC) and field-cooled (FC) conditions in an applied field of 0.1 T over the temperature range 2–300 K using a Quantum Design MPMS XL SQUID magnetometer. The sample was placed into a diamagnetic gelatin capsule, and the data were corrected by extracting the contribution from diamagnetic ionic susceptibilities.

### 2.6. Faraday rotation measurement

The Faraday rotation of the STS-3 single crystal in the direction of the  $c$  axis was measured by the extinction method [24] with two lasers emitting at three wavelengths 532, 633, and 1064 nm at room temperature. A commercial TGG crystal, grown by TCT Co., Ltd. Fuzhou, was used as the standard sample to correct the magnetic field. The magnetic field intensity could be adjusted from 0 to 1.2 T continuously. In order to give detailed information about optical quality of samples, their extinction ratio in the absence of magnetic field were measured by using laser diodes with 1064 nm wavelength at room temperature, and the test results are listed in Table 1.

Download English Version:

<https://daneshyari.com/en/article/1494146>

Download Persian Version:

<https://daneshyari.com/article/1494146>

[Daneshyari.com](https://daneshyari.com)